AIP | The Journal of Chemical Physics

Molecular ordering of PAH/MA-co-DR13 azopolymer layer-by-layer films probed by second-harmonic generation

Heurison S. Silva, Fábio J. S. Lopes, and Paulo B. Miranda

Citation: The Journal of Chemical Physics **145**, 104902 (2016); doi: 10.1063/1.4962341
View online: http://dx.doi.org/10.1063/1.4962341
View Table of Contents: http://scitation.aip.org/content/aip/journal/jcp/145/10?ver=pdfcov
Published by the AIP Publishing

Molecular ordering of PAH/MA-co-DR13 azopolymer layer-by-layer films probed by second-harmonic generation

Heurison S. Silva,[1] Fábio J. S. Lopes,[2] and Paulo B. Miranda[3,4,5,a)]
[1]*Universidade Federal do Piauí – Campus Universitário Ministro Petrônio Portella, Bairro: Ininga, CEP: 64049-550 Teresina, PI, Brazil*
[2]*Universidade de São Paulo, Instituto de Pesquisa Energética e Nucleares, Cidade Universitária-IPEN, Av. Lineu Prestes 2242, CEP: 05508-000 São Paulo, SP, Brazil*
[3]*Instituto de Física de São Carlos, Universidade de São Paulo, Caixa Postal: 369, CEP: 13566-590 São Carlos, SP, Brazil*
[4]*Dipartimento di Fisica, Politecnico di Milano, Piazza Leonardo da Vinci 32, 20132 Milano, Italy*
[5]*Center for Nano Science and Technology @PoliMi, Istituto Italiano di Tecnologia, Via Pascoli 70/3, 20133 Milano, Italy*

(Received 19 July 2016; accepted 24 August 2016; published online 13 September 2016)

Molecular orientation within azopolymer thin films is important for their nonlinear optical properties and photonic applications. We have used optical second-harmonic generation (SHG) to study the molecular orientation of Layer-by-Layer (LbL) films of a cationic polyelectrolyte (poly(allylamine hydrochloride)) and an anionic polyelectrolyte containing azochromophore side groups (MA-co-DR13) on a glass substrate. The SHG measurements indicate that there is a preferential orientation of the azochromophores in the film, leading to a significant optical nonlinearity. However, both the signal strength and its anisotropy are not homogeneous throughout the sample, indicating the presence of large orientational domains. This is corroborated with Brewster angle microscopy. The average SHG signal does not increase with film thickness, in contrast to some reports in the literature, indicating an independent orientational order for successive bilayers. Analyzing the SHG signal as a function of the input and output polarizations, a few parameters of the azochromophore orientational distribution can be deduced. Fitting the SHG signal to a simple model distribution, we have concluded that the chromophores have an angular distribution with a slight in-plane anisotropy and a mean polar angle ranging from 45° to 80° with respect to substrate normal direction, with a relatively large width of about 25°. These results show that SHG is a powerful technique for a detailed investigation of the molecular orientation in azopolymer LbL films, allowing a deeper understanding of their self-assembling mechanism and nonlinear optical properties. The inhomogeneity and anisotropy of these films may have important consequences for their applications in nonlinear optical devices. *Published by AIP Publishing.* [http://dx.doi.org/10.1063/1.4962341]

INTRODUCTION

Multilayered and ultrathin films of water-soluble polymers are very interesting and promising in many technological areas, such as organic diodes,[1,2] optical storage,[3,4] drug delivery,[5] chemical sensors,[6] biosensors,[7,8] and nanobiosensors,[9] to name a few. The Layer-by-Layer (LbL) electrostatic method is a versatile process for obtaining a variety of layered structures of organic compounds with the nanometric control of thickness and composition.[10] In this method, the electrostatic interaction is the driving force for adsorption of polyelectrolyte molecules at the solution/solid interface, leading to multilayered structures on a solid substrate of any shape, including colloidal particles.[11] Therefore, polyelectrolyte multilayer thin films have been investigated on a microscopic level in order to probe, quantify, and control the film properties.[10–13]

Adding chromophores to the polymer backbone and/or as side chains is an important strategy to confer nonlinear optical (NLO) activity to polyelectrolyte LbL films.[14–16] The film structure and the orientational ordering of chromophores can be adjusted by several parameters (polyelectrolyte concentration, pH and ionic strength of the solution, substrate type, and temperature, to name a few), and optical Second-Harmonic Generation (SHG) is a convenient tool to analyze these changes as a function of fabrication parameters. It has been widely used to investigate the average alignment of azo-chromophores in nonlinear optical (NLO) organic films produced by different strategies, such as poled polymer films,[16–19] LbL films,[20–25] Langmuir-Blodgett (LB) films,[26–29] and covalently bonded self-assembled mono-[30] and multilayers.[14,31–33] Besides probing the orientation of chromophores, SHG can also be used to study the kinetics of adsorption.[34–36]

Most previous studies in azopolymer LbL films[20–25] measure SHG versus film thickness to assess if the chromophore orientation is maintained as the number of layers increases, correlating fabrication parameters and

a)Author to whom correspondence should be addressed. Electronic mail: miranda@ifsc.usp.br. Telephone: +55 16 3373 9825. FAX: +55 16 3371 5365.

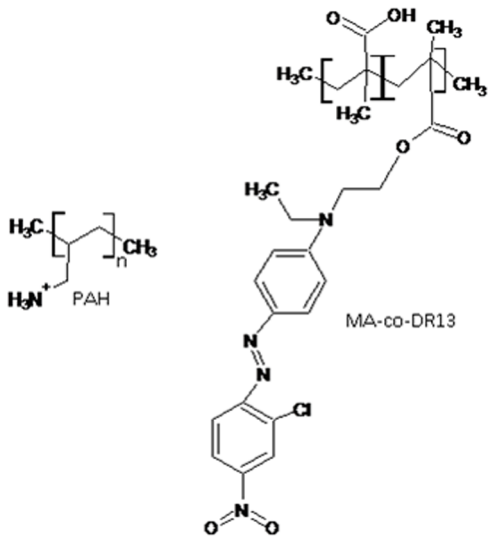

FIG. 1. Structure of the polyelectrolytes used in this work, PAH and MA-co-DR13.

procedures to the film NLO activity, but without a detailed analysis of the molecular orientation in these films. Here we use the polarization dependence and anisotropy of the SHG intensity to quantitatively determine the molecular orientational distribution of Disperse Red 13 (DR13) azogroups in LbL films of the optically inert polyelectrolyte poly(allylamine hydrochloride)—PAH—and the azopolymer methacrylic acid-co-DR13 (MA-co-DR13), whose structures are shown in Figure 1. Although a similar quantitative analysis has been performed for azo-chromophores in LB films,[26,28,29] spin-coated films,[17,18] and self-assembled monolayers,[30] to the best of our knowledge it has not been fully applied to LbL films of azopolymers. We have also investigated how the average orientational distribution changes with film thickness and have shown that the second-order susceptibility does not increase linearly with the number of bilayers, in contrast to what is reported in the literature for some covalently bonded multilayers,[31,32] LB,[37,38] and LbL films.[21,39] Another interesting finding is the presence of large (~mm) molecular orientational domains, which are supported by Brewster Angle Microscopy (BAM) measurements.

MATERIALS AND METHODS

Sample preparation

We have prepared LbL films of poly(allylamine hydrochloride)—PAH (*Aldrich*, M_W = 70 000) and MA-co-DR13 (synthesized according to the procedure of Ref. 49, M_W = 101 700), whose chemical structures are shown in Figure 1. The glass substrates were 5 mm thick for easily separating the top and bottom reflections of the input laser beam, so that only the LbL film on the top surface of the substrate is measured by SHG. They were thoroughly cleaned with a H_2SO_4/HNO_3 mixture (1:1 vol/vol), rinsed extensively with ultrapure water, and blow-dried with N_2 gas right before LbL assembly. All assembly and rinsing solutions were prepared using ultra-pure water (Milli-Q), with resistivity higher than 18 MΩ · cm, and had concentrations of 0.8 mg/ml for PAH and 0.5 mg/ml for MA-co-DR13, both with pH 10 adjusted by adding NH_4OH solutions. Each adsorption step was set to 3 min, followed by rinsing in an NH_4OH solution of pH 10 for 1 min and blow-drying with N_2 gas. These steps were repeated until the desired number of bilayers was attained.

Second-harmonic generation analysis

Second-harmonic generation (SHG) arises from a polarization that oscillates at a frequency 2ω, when only one electric field at frequency ω is applied. This nonlinear optical process is a result of a second-order nonlinear susceptibility, $\chi^{(2)}$, as shown in the following:

$$\vec{P}^{(2)}(2\omega = \omega + \omega) = \overleftrightarrow{\chi}^{(2)} : \vec{E}(\omega)\vec{E}(\omega) \quad (1)$$

As a polar third-rank tensor, $\chi^{(2)}$ changes sign under the inversion operation (in the electric dipole approximation), so that in centrosymmetric media $\chi^{(2)} = 0$. Therefore, no second-order optical process is possible in media with inversion symmetry, so that SHG is intrinsically sensitive to their surfaces and interfaces, where the inversion symmetry is necessarily broken. Most bulk molecular materials do have inversion symmetry, because the functional groups are, in general, randomly or oppositely oriented.[26] For the specific case of thin polymeric films adsorbed on solid substrates, such as Layer-by-Layer films, if asymmetric molecules (or functional groups) adsorb with random orientations, the net SHG signal is canceled out. Conversely, if there is a substantial SHG signal, we can conclude that molecules have a net average orientation in the film. More detailed considerations about the importance of symmetry on the interpretation of SHG (and other second-order processes, such as Sum-Frequency Generation—SFG) can be found elsewhere.[40–43]

For second-harmonic generation at interfaces between two different media, Shen demonstrated that the intensity of the second-harmonic signal is given by[40,42]

$$I(2\omega) = \frac{8\pi^3 (2\omega)\sec^2\theta}{c^3\hbar[\varepsilon_1(2\omega)]^{1/2}\varepsilon_1(\omega)}\left|\hat{e}(2\omega)\cdot\overleftrightarrow{\chi}_s^{(2)}:\hat{e}(\omega)\hat{e}(\omega)\right|^2 I^2(\omega), \quad (2)$$

where the SHG signal is expressed in terms of the effective second-order susceptibility of the surface $\chi_s^{(2)}$. The macroscopic susceptibility $\chi_{ijk}^{(2)}$ is related to microscopic molecular hyperpolarizability $\beta_{\alpha\beta\gamma}$ through an orientational average of a coordinate transformation, where $\beta_{\alpha\beta\gamma}$ is a tensor that relates the components of dipole moment $\vec{p}(2\omega)$ of molecule to local electric-field components, $\vec{E}_{local}(\omega)$.

For chromophores with delocalized electrons mainly along a single direction (such as the azobenzene moiety in MA-co-DR13—see structure in Figure 1), the hyperpolarizability $\beta_{\alpha\beta\gamma}$ will have only one dominant element, $\beta_{\xi\xi\xi}$, along the molecular axis ξ, as shown in Figure 2. In this case, the relation between $\chi_{ijk}^{(2)}$ and $\beta_{\alpha\beta\gamma}$ for a molecular thin film adsorbed on the surface is given by Eq. (3), where the brackets represent an average over the chromophore

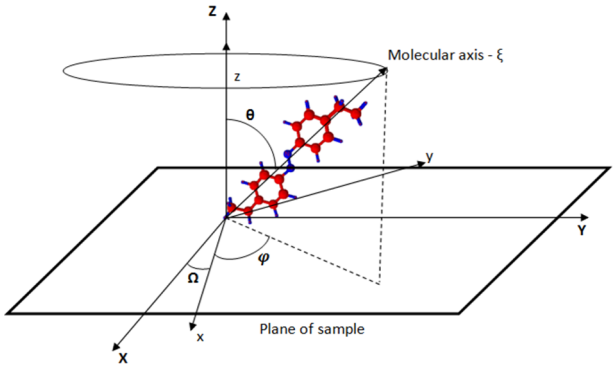

FIG. 2. Molecular geometry with the azobenzene group (Ph–N = N–Ph) along the ξ axis. The frame (x, y, z) is the sample reference frame, with xz as a mirror plane. The (X, Y, Z) frame is the laboratory coordinate system, with XZ as the incidence plane. The molecule is tilted by the polar angle θ with respect to the surface normal, and φ is the azimuthal angle with respect to the sample symmetry direction, which in turn is rotated by Ω with respect to the incidence plane (X direction).

orientational distribution function,

$$\chi^{(2)}_{ijk} = N\left\langle\left(\hat{i}\cdot\hat{\xi}\right)\left(\hat{j}\cdot\hat{\xi}\right)\left(\hat{k}\cdot\hat{\xi}\right)\right\rangle\beta_{\xi\xi\xi}. \tag{3}$$

Since the transformation of coordinates from the molecular frame $\hat{\alpha}$, $\hat{\beta}$ and $\hat{\gamma}$ to the sample frame $\hat{i}$, $\hat{j}$ and $\hat{k}$ is given by

$$\hat{i}\cdot\hat{\xi} = \sin\theta\cos\varphi, \tag{4}$$

$$\hat{j}\cdot\hat{\xi} = \sin\theta\sin\varphi, \tag{5}$$

$$\hat{k}\cdot\hat{\xi} = \cos\theta, \tag{6}$$

and considering a thin film with a C_{1v} symmetric distribution of chromophores on the plane *xy* (*xz* is the sample plane of symmetry), we obtain six independent elements of the tensor $\chi^{(2)}_{ijk}$,[52]

$$\chi_1 = \chi^{(2)}_{zzz} = N\left\langle\cos^3\theta\right\rangle\beta_{\xi\xi\xi}, \tag{7}$$

$$\chi_2 = \chi^{(2)}_{xxx} = N\left\langle\sin^3\theta\cos^3\varphi\right\rangle\beta_{\xi\xi\xi}, \tag{8}$$

$$\chi_3 = \chi^{(2)}_{yyz} = \chi^{(2)}_{zyy} = \chi^{(2)}_{yzy} = N\left\langle\left(\cos\theta-\cos^3\theta\right)\left(1-\cos^2\varphi\right)\right\rangle\beta_{\xi\xi\xi}, \tag{9}$$

$$\chi_4 = \chi^{(2)}_{xxz} = \chi^{(2)}_{zxx} = \chi^{(2)}_{xzx} = N\left\langle\left(\cos\theta-\cos^3\theta\right)\cos^2\varphi\right\rangle\beta_{\xi\xi\xi}, \tag{10}$$

$$\chi_5 = \chi^{(2)}_{xzz} = \chi^{(2)}_{zxz} = \chi^{(2)}_{zzx} = N\left\langle\left(\sin\theta-\sin^3\theta\right)\cos\varphi\right\rangle\beta_{\xi\xi\xi}, \tag{11}$$

$$\chi_6 = \chi^{(2)}_{xyy} = \chi^{(2)}_{yxy} = \chi^{(2)}_{yyx} = N\left\langle\left(\cos\varphi-\cos^3\varphi\right)\sin^3\theta\right\rangle\beta_{\xi\xi\xi}. \tag{12}$$

Therefore, measuring these six elements in the above equations allows determining up to five parameters of the orientation distribution function of the adsorbed monolayer (since usually the product $N\beta_{\xi\xi\xi}$ is unknown). This can be performed by SHG measurements with several combinations of polarization, such as SS, SP, PS, PP, MS, MP, where the first polarization is for the pump beam at ω and the other is for the generated beam at 2ω. S indicates the polarization with the electric field perpendicular to the incidence plane, and P is with the electric field parallel to the incidence plane. M polarization is that where the electric field has equal components perpendicular and parallel to the incidence plane (mixed polarization). We should note, however, that in general the laboratory coordinate system (XYZ), defined by incidence plane XZ and the sample plane XY, is not coincident with the sample coordinate system (xyz), defined by the sample plane xy and the plane of symmetry xz. We define the angle Ω describing the relation between the two coordinate systems, as shown in Figure 2.

Therefore, to fully determine $\chi^{(2)}_{eff}$ in laboratory frame, we need to do an additional coordinate transformation from the sample frame (xyx) to the laboratory frame (XYZ), rotated by an angle Ω. Thus, we obtain $\chi^{(2)}_{eff}$ for six polarization combinations as a function of Ω and the independent components χ_1 to χ_6 (Equations (7)–(12)), which in turn depend on the orientational distribution of the chromophores: $\chi^{(2)}_{eff,SS}(\Omega)$, $\chi^{(2)}_{eff,SP}(\Omega)$, $\chi^{(2)}_{eff,PP}(\Omega)$, $\chi^{(2)}_{eff,MS}(\Omega)$, $\chi^{(2)}_{eff,MP}(\Omega)$. The complete functional form for these nonlinear susceptibilities as a function of χ_1–χ_6 can be found elsewhere.[44,45]

In practice, SHG measurements consist in recording the SH intensity as a function of the sample azimuthal angle Ω for several polarization combinations. From them, we can determine the independent components, from χ_1 to χ_6, that are related to the orientational distribution of molecules on the sample. For example, in the case of an isotropic sample on its *xy* plane, only χ_1 and $\chi_3 = \chi_4$ will be nonvanishing, so that all $\chi^{(2)}_{eff}$ are either null or independent of azimuthal angle Ω, as expected. In this case, the ratio $\frac{\chi_1}{\chi_3} = \frac{\langle\cos^3\theta\rangle}{\langle\cos\theta-\cos^3\theta\rangle}$ depends only on the average molecular tilt with respect to the normal direction (polar angle θ). Therefore, measurements can be qualitatively interpreted to immediately determine if samples are isotropic or not about the surface, and if polar orientation changes significantly.

In order to fully determine the orientation of chromophores in the film, we assume that this orientation is described by the following distribution function:[27,46–48]

$$F(\theta,\varphi) = A\left(e^{-\frac{(\theta-\theta_0)^2}{2\sigma^2}}\right)\left[d_0 + d_1\cos(\varphi) + d_2\cos(2\varphi) + d_3\cos(3\varphi)\right]. \tag{13}$$

The first term of $F(\theta,\varphi)$ is a Gaussian distribution function for the polar angle θ, where θ_0 is the average molecular tilt with respect to the z-axis and σ is the polar distribution width. *A* is a normalization constant, given as follows:

$$A = \frac{1}{(2\pi)^{1/2}\sin(\theta_0)\,\sigma\left(1-\frac{\sigma^2}{2}\right)}. \tag{14}$$

The second factor in Equation (13) is a Fourier series on the azimuthal angle φ, truncated at the third term, where d_0 is the normalization constant equal to $1/2\pi$. A parameter d_1 describes a forward-backward asymmetry in the azimuthal distribution, where a positive value indicates more molecules oriented along $\varphi = 0$ than in the opposite direction, $\varphi = 180°$. The parameter d_2 gives the anisotropy about the xz mirror plane, with a positive d_2 indicating more chromophores aligned along the x axis than along the y axis. Finally, d_3 yields an anisotropy with three-fold symmetry. Therefore, the term

in square brackets in Eq. (3) describes the overall anisotropy of the chromophores along the sample plane, with respect to the mirror plane xz. In order to obtain the parameters of the orientational distribution function $F(\theta,\varphi)$, we need to experimentally measure $\chi^{(2)}_{eff}(\Omega)$ in the six polarization combinations as the sample is rotated (varying the sample azimuthal angle Ω). We then adjust the data (simultaneous fitting) to the corresponding equations for $\chi^{(2)}_{eff}(\Omega)$ with each polarization combination in order to find the numerical values for χ_1–χ_6 (Equations (7)–(12))), which in turn depend on the parameters θ_0, σ, d_1, d_2, and d_3, as well as the initial sample azimuth Ω_0 (initial angle between sample symmetry x-axis and the X-axis in the laboratory frame—see Figure 2). The six equations, Eqs. (7)–(12) are then solved to get the parameters of $F(\theta,\varphi)$.

SHG setup

The second-harmonic measurements were performed with a Q-switched mode-locked Nd^{+3}:YAG laser (Coherent, Inc., Antares 76), producing pulse trains of ~20 mode-locked pulses of 100 ps duration at 1064 nm, separated by 13 ns, with a repetition rate of 100 Hz. The total energy of each pulse train was ~5 mJ, illuminating the sample at a 60° incidence angle, yielding a spot on the surface with a 1.0×2.0 mm diameter. The SHG signal was measured with a photon-counting system based on a gated photomultiplier, after spectral filtering with color filters (Schott's BG39 for SHG output and RG 750 for 1064 nm input). Polarization of the input and output beams was controlled with glan-laser polarizers placed right before and after the color filters, which in turn were the closest components to the sample stage (a mirror mount placed on a 360° rotation stage).

RESULTS AND DISCUSSION

Homogeneity of samples

In order to verify the growth of PAH/MA-co-DR13 LbL films, we have monitored the UV-Vis absorbance due superposition of n-π and π–π* bands of the azochromophore of MA-coDR13. Figure 3 shows the absorbance near the band maximum as a function of the number of PAH/MA-co-DR13 bilayers, from which we can conclude that the amount of polyelectrolyte for each deposited bilayer is not the same. The initial bilayers tend to be thinner, but after the 6th bilayer, the adsorbed amount per bilayer is significantly larger.

Initially we preformed SHG measurements as a function of the azimuthal angle Ω (where Ω = 0 is the sample dipping direction during LbL assembly) for two different spots of the 1 bilayer PAH/MA-co-DR13 film, in order to verify its homogeneity. Results are shown in Figure 4, where it is clear that the SHG signal is anisotropic, which indicates that the DR13 chromophores have a preferential orientation, not only in terms of tilt (polar orientation) but also in the azimuthal distribution. However, both the SHG signal intensity and anisotropy are different for the two spots on the same sample (PAH/MA-co-DR13 bilayer). Repeated measurements of the SHG azimuthal scans on the same spot of the same sample

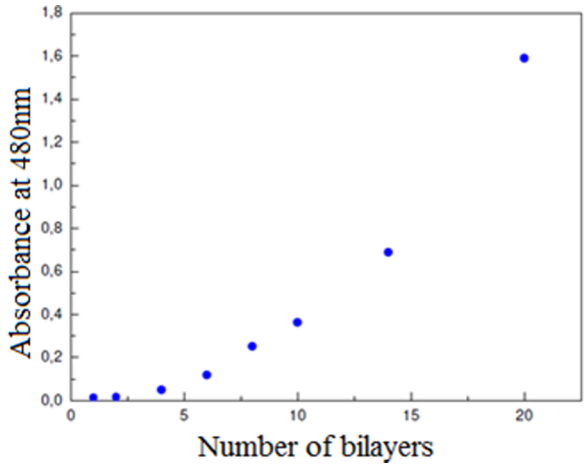

FIG. 3. UV-Vis absorbance at 480 nm, near the absorption band maximum of DR13 azo-chromophores.

did not show any obvious change in the SHG anisotropy pattern, so that we can conclude that the input laser beam is not inducing any gradual change to the molecular orientation (by 2-photon-excited photoisomerization, for example).

Similar behavior was observed for thicker films, such as with four PAH/MA-co-DR13 bilayers (data not shown). This wide variation of SHG signal intensity and anisotropy indicates the inhomogeneity of samples and suggests the presence of orientational domains in these (PAH/MA-co-DR13) films. This conclusion is consistent with data by Anceau *et al.*[26] who confirmed with SHG imaging the existence of these domains in LB monolayers of hemicyanine dyes, showing different SHG signal intensities and polarization dependences in different regions of samples. They are also in agreement with a morphological study of PAH/MA-co-DR13 LbL films using atomic force microscopy measurements by De Sousa *et al.*[49] As show in our previous report on other polyelectrolyte LbL films,[50] this sample inhomogeneity is likely a result of blow-drying them with a N_2 stream, which is a quite common procedure in LbL film fabrication. Thus, in each region of the samples, there are domains in which chromophores have a certain average orientation, but it is different for each domain. When the laser beam impinges on one of these domains or in a region containing some of them, each sample point will generate a different SHG signal intensity and characteristic anisotropy pattern. In contrast, if the domains are very small, so that the illuminated region contains tens of these domains, by rotating the sample, we should not observe variations in the SHG signal, since it would be an average of many domains oriented in random directions. Therefore we can conclude that the domains responsible for the sample inhomogeneity must have dimensions comparable to the size of the laser beam (about 1 mm^2), that is, at least on the order of a few 100 μm in diameter.

This conclusion can be confirmed through Brewster Angle Microscopy (BAM) imaging. These BAM measurements were obtained by focusing a P-polarized laser beam (incident at the Brewster angle of the glass substrate) on the anisotropic sample. Without the film, no reflection should be observed

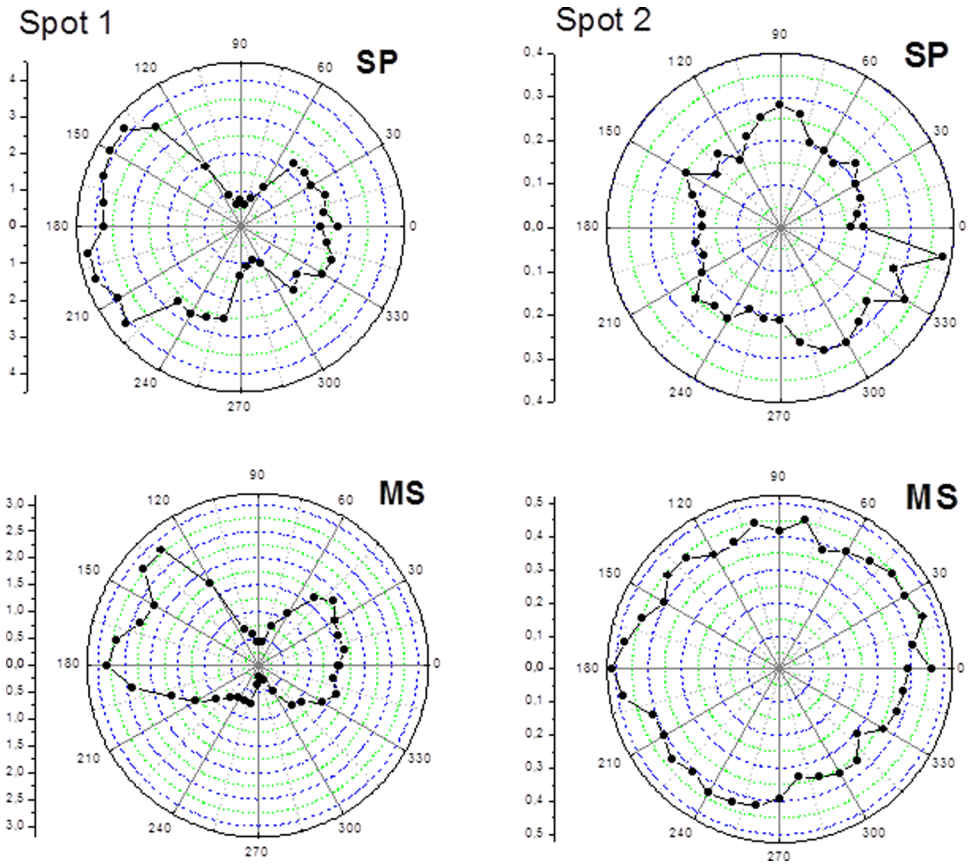

FIG. 4. SHG measurements as a function of angle of rotation Ω for two different spots on the 1 bilayer PAH/MA-co-DR13 film. Left: SP and MS polarization combination on the spot 1. Right: SP and MS polarization combination on the spot 2.

with P polarization, so that the contrast in these images is mainly due to variations of film thickness (and/or density and orientation). Figure 5 shows BAM images, showing the macroscopic domains that are responsible for the inhomogeneity of the SHG intensity and anisotropy, observed at different spots of the samples, and also reported in Ref. 26 for LB films of long-chain hemicyanine molecules with much higher spatial resolution.

Each image in Figure 5 has about 0.178 mm^2. Then, as an estimate, each domain may have an average area of about 0.10 mm^2 or more, while the laser beam spot in SHG measurements had about 1.5 mm^2. Therefore, the fundamental beam illuminates from a few to a few tens of domains with different orientational ordering, generating SHG patterns with a somewhat smaller anisotropy than each individual domain.

SHG measurements

In Figure 6, we show a typical SHG measurement as a function of azimuthal angle Ω of the 10-bilayer sample (taking care to illuminate always the same spot as the sample is rotated) for six polarization combinations of incident and generated beams: SS, SP, MP, MS, PS, and PP, where the first letter refers to the polarization of the input beam and the second to the polarization of the generated beam. It is important to emphasize that a strong SHG signal from the samples is an important result, since this implies that the films have a preferential molecular ordering. On the contrary, if they were disordered films, no SHG signal should be noted.

Besides the data in Figure 6, we have also measured samples with 1, 2, 4, 6, 8, 10, 14, and 20 bilayers. In general, for all films with different numbers of bilayers, the SHG signal is more intense for polarization combinations SP, MS, and MP, while the SHG signal for PS and SS polarization combinations are relatively small or nearly vanishing. However, such non-zero signals are a strong evidence of anisotropic samples, since for perfectly isotropic samples, these PS and SS polarizations combinations should be null.

Orientational distribution of chromophores

In order to determine the orientational distribution of chromophores on samples of self-assembled films of PAH/MA-co-DR13, we preformed the theoretical fitting of the SHG azimuthal scans as described in the section titled "MATERIALS AND METHODS." For determining the orientational distribution of chromophores, we used a distribution function $F(\theta, \varphi)$ as described in Eqs. (13) and (14). A simultaneous adjust of all six curves (one for each polarization combination) was performed with statistical weighting to determine the following seven parameters: Ω_0 (azimuthal angle between the sample symmetry plane and the dipping direction), N_s (an overall multiplicative factor, proportional to the product of $\beta_{\xi\xi\xi}$ and the surface density of adsorbed molecules), θ_0 (center of a Gaussian distribution of polar angles with respect to the surface normal), σ (width of the polar distribution), and d_1, d_2, d_3 (parameters that determine the azimuthal distribution of chromophores, as defined by Eq. (13)).

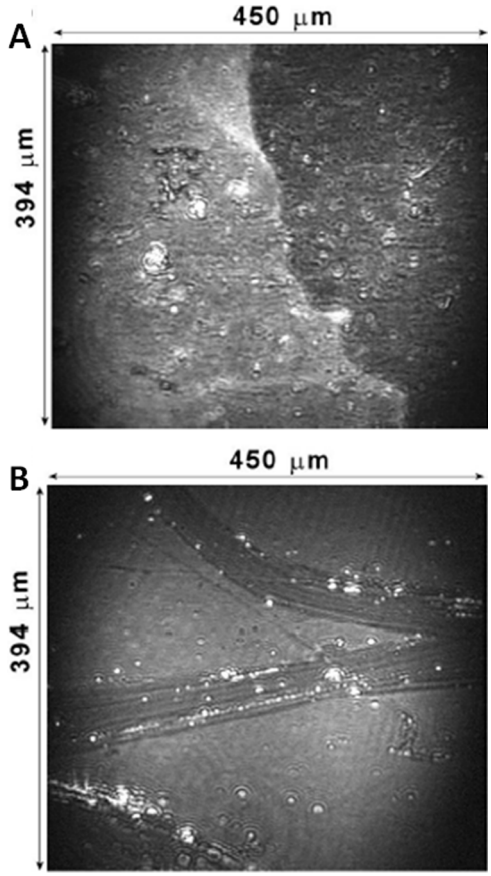

FIG. 5. Brewster angle microscopy images (a) for a 1-bilayer film and (b) for a 4-bilayer (PAH/MA-co-DR13) film.

The best fit for the 10-bilayer film is shown in Figure 6 as colored lines and the fitting parameters are listed in Table I, together with those for samples with different numbers of bilayers. For example, the $F(\theta,\varphi)$ function for the 10-bilayer sample is expressed as $F(\theta,\varphi) = f(\theta)\cdot g(\varphi)$ in order to better visualize the Gaussian distribution of polar angles θ, and the anisotropy in the azimuthal distribution function $g(\varphi)$, which are shown in Figures 6(c) and 6(d). From the fitting curves shown in Figure 6, one may think at first that the quality of the fit is not so good. However, we should emphasize that it is quite difficult to get good fits, since we have only seven adjustable parameters to simultaneously fit all six curves, including their relative magnitudes. A judicious choice of the starting values for each parameter is also important in determining if the fitting will converge to a global minimum or not. We should also note that the intensity ratios between different polarization combinations and the anisotropy of the SHG signal are both very sensitive to the parameter values. Therefore, even with relatively poor fitting curves, the uncertainty in the obtained parameters is not so large, and it is usually smaller than the parameter variability due to sample inhomogeneity. Hence, the error bars in Table I are not obtained from the fitting routine, but estimated from the typical variations in the parameters obtained from data taken at different spots of the sample.

Another source of uncertainty in the quantitative determination of the orientational distribution is the value of the refractive index of the film, which is used in the calculation of the local field inside the film (Fresnel factors that are used to calculate $\chi_s^{(2)}$ in Eq. (2)),[51] since we do not know precisely the refractive index of an azodye monolayer.[52] It is common to use the refractive index of the substrate as refractive index value of the interface (n'), which in our case is 1.519 at 532 nm and 1.507 at 1064 nm. But this may not be a good approximation because the fits and final values of parameters are very sensitive to refractive index of the interface.[51] Initially, we used for it the value 1.225, based on a model proposed by Zhuang *et al.*,[51] but this value should be appropriate only for molecules at the interface between two different media (here, glass and air), which is not the case for self-assembled films with more than one bilayer. Therefore, we decided to use the value 1.5 (close to that for the substrate and bulk polymer films) for the refractive index of the LbL films with any number of bilayers.

From these results, it is possible to observe in Figures 6(c) and 6(d) the preferential orientation and anisotropy for the 10-bilayer film. The polar distribution $f(\theta)$ is reasonably wide ($\sigma \cong 25°$), but centered at around 50°, so that the final distribution is a truncated Gaussian in the 0°–180° interval. Although this distribution suggests that chromophores are aligned along an average polar direction $\theta_0 \cong 50°$, we should note that chromophores with supplementary polar orientations θ_0 and (180°- θ_0) generate the same SHG signal, since their $\chi^{(2)}$ differ only by a change in sign. For now, we cannot determine if chromophores are pointing upward or downward, with an average angle θ_0 with respect to the normal direction. In principle, this ambiguity could be solved through phase measurements between SHG signals from the film and a reference sample, such as crystalline quartz.[53,54] However, this experiment is not essential for our interpretation of the SHG results. Regarding the azimuthal distribution, we see that the main contribution to the anisotropy is given by the parameter d_2, with d_1 and d_3 being significantly smaller. However, the value of d_2 (=−0.017) is also small compared with d_0 (=0.159), implying a slight anisotropy (elliptical azimuthal distribution g(φ) with major axis along $\Omega_0 = -11.9°$), with also very little forward-backward asymmetry (d_1). Finally, we note that since the samples were not poled with an artificial method like photo alignment, we can conclude that this spontaneous preferential ordering is due to electrostatic interactions and the effects of N_2 flow drying[50] during to the LbL fabrication process. This explains why the sample symmetry direction Ω_0 varies so much from sample-to-sample (and spot-to-spot), since it is mainly due to the drying procedure and is unrelated to the sample dipping direction.

Chromophore orientation vs. film thickness

In order to verify how the molecular ordering changes as the films grow, the fitting parameters to the SHG data for films with varying numbers of bilayers are displayed in Figure 7. As we can see, SHG intensity (roughly proportional to N_S^2) does not grow as a function of number of bilayers. If all bilayers had the same average orientation, N_s should have increased linearly with thickness and the SHG signal would be proportional to the square of the number of bilayers. However, we can see that N_s fluctuates widely around an

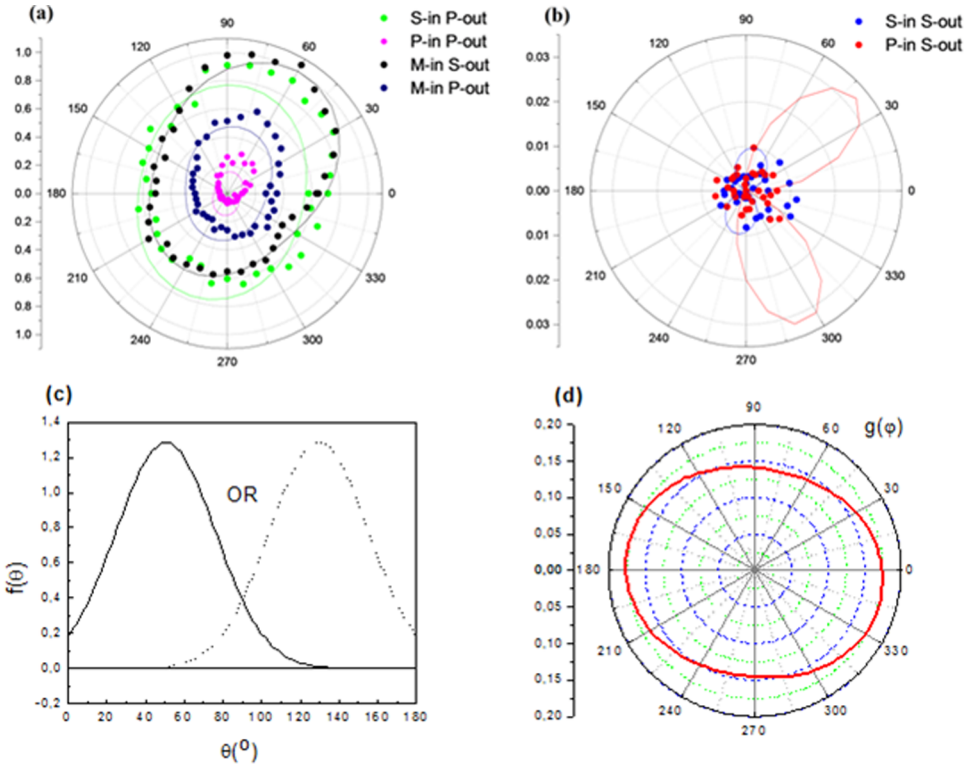

FIG. 6. Panels (a) and (b): SHG signal intensity as a function of azimuthal angle Ω for a 10-bilayer LbL film of PAH/MA-co-DR13 for six polarizations combinations. Solid lines are fits to the data, as described in the section titled "MATERIALS AND METHODS." (c) Polar and (d) azimuthal angle distributions of DR13 chromophores, as determined from the fitting parameters.

average value of ~90. Indeed, it is possible to note in Figure 7 the uncertainty in the parameters associated with the inhomogeneity of samples, as seen in samples with 1, 4, 6, 8, and 14 bilayers, for which we have fitted two sets of SHG measurements acquired in different spots of the samples. This average variability due to inhomogeneity is around 17% for N_s, 8% for θ_0, 3% for σ, and 57% for d_i. Within these uncertainties, there is no apparent trend of the parameters as a function of number of bilayers, with θ_0 varying from 45° to 80°, σ ~ 25°, and $|d_2|$ approximately in the 0.006–0.065 range (with d_1 and d_3 much smaller than that). Therefore, we can conclude that each layer does not have the same molecular orientation (possibly acquired upon adsorption) as the number of bilayers increases.

In fact, a likely explanation for the roughly constant SHG intensity with increasing film thickness would be due to this film inhomogeneity described above: each layer is composed of orientational domains, whose orientations are independent from each other, both within each layer and also among different layers. In this case, chromophores in each domain acquire a non-random molecular orientation, generating an SHG signal. However, this average molecular orientation for each domain, being independent of each other, would lead to SHG signals from each layer that can interfere constructive or destructively, resulting in a variable intensity around an average value as film thickness increases.

Alternatively, another explanation for why the optical nonlinearity does not increase with film thickness could be due to the SHG signal being generated only by the first bilayer of each sample, which varies from point to point because of the film inhomogeneity. In this picture, the first bilayer would be ordered due to an interaction with the substrate, and the subsequent bilayers would be completely disordered, not generating any additional SHG signal because their chromophores would have random orientations. Such centrosymmetric orientation could be due electrostatic interactions between the azopolymer layer and the adjacent PAH layers, as reported in our previous paper.[54] However, we can rule out this explanation by comparing the SHG anisotropy for samples with 1 and many bilayers. If this picture were correct, the SHG anisotropy would not have changed significantly as the films became thicker. In

TABLE I. Values for the seven parameters obtained from simultaneous fitting the SHG measurements as a function of polarization and sample azimuth.

Number of bilayers	Ω_0	N_s	θ_0	σ	d_1	d_2	d_3
1	41.4 ± 7.7	89.0 ± 6.4	51.1 ± 0.2	23.3 ± 0.3	0.0036 ± 0.000 2	−0.029 ± 0.014	−0.0003 ± 0.0002
2	23.6 ± 8.6	47.6 ± 8.1	44.0 ± 3.7	33.9 ± 0.8	−0.0001 ± 0.000 05	0.015 ± 0.008	0.0019 ± 0.0014
4	−21.7 ± 3.1	44.0 ± 2.4	68.1 ± 10.2	22.2 ± 1.8	0.0037 ± 0.001 4	−0.054 ± 0.023	0.0026 ± 0.0014
6	3.1 ± 10.3	137 ± 15	75.0 ± 1.8	21.4 ± 0.2	0.0002 ± 0.000 1	−0.030 ± 0.020	−0.0026 ± 0.0014
8	4.9 ± 8.5	133 ± 26	82.4 ± 7.7	23.6 ± 0.1	0.0017 ± 0.001 2	0.065 ± 0.061	−0.002 ± 0.002
10	−11.9 ± 4.9	75.9 ± 12.9	50.4 ± 4.2	25.7 ± 0.6	−0.0031 ± 0.001 4	−0.017 ± 0.009	−0.0005 ± 0.0004
14	50.6 ± 3.6	116 ± 47	73.2 ± 10.4	21.1 ± 0.4	0.0008 ± 0.000 6	0.0023 ± 0.003	−0.0001 ± 0.0001
20	23.2 ± 9.0	103 ± 18	70.8 ± 5.9	22.8 ± 0.6	0.0006 ± 0.000 3	0.006 ± 0.003	−0.0015 ± 0.0011

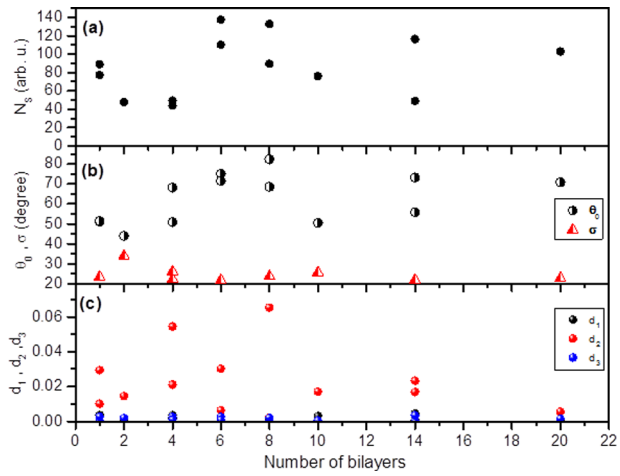

FIG. 7. Fitting parameters for the chromophore angular distribution functions for samples with varying number of bilayers, using data from Table I. (a) Effective chromophore surface density N_s. (b) Parameters θ_0 and σ of the Gaussian distribution f(θ) of the polar angle θ. (c) Parameters d_1, d_2, and d_3, for the azimuthal distribution function g(φ).

contrast, the azimuthal SHG plots (not shown) indicate that the typical SHG signal anisotropy is considerably reduced as the number of bilayers increases, implying that successive bilayers contribute to the net SHG signal. However, this reduction of anisotropy in thicker samples is not quite evident in Figure 7 from the variations of d_1, d_2, and d_3 parameters as a function of number of bilayers. As commented above, this is partly due to the difficulty in fitting the SHG data to extract reliable parameters, and to the large parameter uncertainty from sample inhomogeneity, which prevents seeing a clear trend as a function of number of bilayers, since only a limited amount of SHG data was fitted.

Therefore, based on the SHG measurements as a function of LbL film thickness, we propose that chromophores in each bilayer have a non-random molecular orientation within large (∼100 μm) orientational domains which are independent of each other, leading to destructively and constructively contributions from each bilayer to the net SHG signal of multilayer LbL films. This yields an SHG signal that does not grow with film thickness, and to a small anisotropy of chromophores (along a certain direction, but forward and backward are equivalent, dominated by the parameter d_2) that decreases as the number of bilayers increases.

CONCLUSIONS

In this work, we applied second-harmonic generation (SHG) to study the molecular orientation of the azopolymer MA-co-DR13 in self-assembled Layer-by-Layer (LbL) films with the polyelectrolyte PAH. The presence of SHG signals is a strong evidence of a net molecular orientation, with a non-random orientational distribution of chromophores. Molecular orientation was determined by fitting the polarization-dependent SHG anisotropy measurements to a model orientational distribution function. The average polar angle was found to range from 45° to 80° with respect to substrate normal direction, with a relatively wide polar angle distribution (σ ∼ 25°). Azimuthal anisotropy was small, but nonvanishing. It was observed that the average SHG signal intensity does not increase systematically with the number of bilayers, in contrast to some reports for self-assembled multilayers,[31,32] Langmuir-Blodgett,[37,38] and LbL films,[21,39] indicating that the molecular ordering of each layer is independent of the other ones. We also found that the molecular ordering in these LbL films is inhomogeneous, in both polar and azimuthal distributions. Brewster-angle microscopy images confirmed the presence of large domains (∼100 μm) that are likely induced by the blow-drying of the films.[50] These results show that SHG is a powerful technique for a detailed investigation of the molecular orientation in azopolymer LbL films, allowing a deeper understanding of their self-assembling mechanism and nonlinear optical properties. The inhomogeneity and anisotropy of these films may have important consequences for their applications in nonlinear optical devices.

ACKNOWLEDGMENTS

This work was supported by the Brazilian agencies FINEP, CAPES, FAPESP, and CNPq.

[1]D. Delongchamp and P. T. Hammond, "Layer-by-Layer assembly of PEDOT/polyaniline electrochromic devices," Adv. Mater. **13**, 1455–1459 (2001).
[2]S. Roy, S. Kundu, S. K. Roy, and A. J. Pal, "Impedance characteristics of layer-by-layer electrostatic self-assembled films of evans blue," Mater. Chem. Phys. **77**, 784–790 (2002).
[3]V. Zucolotto, P. J. Strack, F. R. Santos, D. T. Balogh, C. J. L. Constantino, C. R. Mendonca, and O. N. Oliveira, Jr., "Molecular engineering strategies to control photo-induced birefringence and surface-relief gratings on layer-by-layer films from an azopolymer," Thin Solid Films **453**, 110–113 (2004).
[4]Q. Ferreira, P. A. Ribeiro, O. N. Oliveira, Jr., and M. Raposo, "Long-term stability at high temperatures for birefringence in PAZO/PAH layer-by-layer films," Appl. Mater. Interfaces **4**, 1470–1477 (2012).
[5]B. G. Geest, C. Déjugnat, E. Verhoeven, G. B. Sukhorukov, A. M. Jonas, J. Plain, J. Demeester, and S. C. Smedt, "Layer-by-layer coating of degradable microgels for pulsed drug delivery," J. Controlled Release **116**, 159–169 (2006).
[6]A. Riul, Jr., D. S. Dos Santos, Jr., K. Wohnrath, R. Di Tommazo, A. C. P. L. F. Carvalho, F. J. Fonseca, O. N. Oliveira, Jr., D. M. Taylor, and L. H. C. Mattoso, "Artificial taste Sensor: Efficient combination of sensors made from Langmuir–Blodgett films of conducting polymers and a ruthenium complex and self-assembled films of an azobenzene-containing polymer," Langmuir **18**, 239–245 (2002).
[7]T. Hoshi, N. Sagae, K. Daikuhara, and J.-I. Anzai, "Multilayer membranes via layer-by-layer deposition of ascorbate oxidase and Au nanoparticles on the Pt electrode for reduction of oxidation current derived from ascorbate," Talanta **71**, 644–647 (2007).
[8]M. D. Shirsat, C. O. Too, and G. G. Wallace, "Amperometric glucose biosensor on layer by layer assembled carbon nanotube and polypyrrole multilayer film," Electroanalysis **20**, 150–156 (2008).
[9]A. C. N. Silva, D. K. Deda, C. C. Bueno, A. S. Moraes, A. L. Roz, F. M. Yamaji, R. A. Prado, V. Viviani, O. N. Oliveira, Jr., and F. L. Leite, "Nanobiosensors exploiting specific interactions between an enzyme and herbicides in atomic force spectroscopy," J. Nanosci. Nanotechnol. **14**, 6678–6684 (2014).
[10]K. Ariga, Y. Yamauchi, G. Rydzek, Q. Ji, Y. Yonamine, K. C.-W. Wu., and J. P. Hill, "Layer-by-layer nanoarchitectonics: Invention, innovation, and evolution," Chem. Lett. **43**, 36–68 (2014).
[11]I. L. Radtchenko, G. B. Sukhorukov, S. Leporatti, G. B. Khomutov, E. Donath, and H. Möhwald, "Assembly of alternated multivalent ion/polyelectrolyte layers on colloidal particles. Stability of the multilayers and encapsulation of macromolecules into polyelectrolyte capsules," J. Colloid Interface Sci. **230**(2), 272–280 (2000).

[12]C. M. Daikuzono, C. A. R. Dantas, D. Volpati, C. J. L. Constantino, M. H. O. Piazzetta, A. L. Gobbi, D. M. Taylor, O. N. Oliveira, Jr., and A. Riul, Jr., "Microfluidic electronic tongue," Sens. Actuators, B **207**, 1129–1135 (2015).
[13]L. M. Sáiz, I. A. Zucchi, P. A. Oyanguren, M. J. Galante, R. C. Sanfelice, D. T. Balogh, and O. N. Oliveira, Jr., "Effect of molecular architectures in photoinduced birefringence in films of azo-modified diblock copolymers," Opt. Mater. **37**, 816–822 (2014).
[14]E. H. Kang, T. Bu, P. Jin, J. Sun, Y. Yang, and J. Shen, "Layer-by-layer deposited organic/inorganic hybrid multilayer films containing noncentrosymmetrically orientated azobenzene chromophores," Langmuir **23**, 7594–7601 (2007).
[15]K. Yang, S. Balasubramanian, X. Wang, J. Kumar, and S. Tripathy, "Electroabsorption spectroscopy study of an azopolymer film fabricated by electrostatic adsorption," Appl. Phys. Lett. **73**, 3345–3347 (1998).
[16]S. Bauer, "Poled polymers for sensors and photonic applications," J. Appl. Phys. **80**, 5531–5558 (1996).
[17]T. Shioda, D. H. Chung, Y. Takanishi, K. Ishikawa, B. Park, and H. Takezoe, "Axial and polar orientational changes by rubbing/photoalignment processes in a liquid crystal alignment layer studied by optical second-harmonic generation," Jpn. J. Appl. Phys., Part 1 **40**, 2387–2390 (2001).
[18]V. Rodriguez, F. Lagugné-Labarthet, and C. Sourisseau, "Orientation distribution functions based upon both ⟨P1⟩, ⟨P3⟩ order parameters and upon the four ⟨P1⟩ up to ⟨P4⟩ values: Application to an electrically poled nonlinear optical azopolymer film," Appl. Spectrosc. **59**, 322–328 (2005).
[19]R. D. Schaller, R. J. Saykally, Y. R. Shen, and F. Lagugné-Labarthet, "Poled polymer thin-film gratings studied with far-field optical diffraction and second-harmonic near-field microscopy," Opt. Lett. **28**, 1296–1298 (2003).
[20]S.-H. Lee, S. Balasubramanian, D. Y. Kim, N. K. Viswanathan, S. Bian, J. Kumar, and S. K. Tripathy, "Azo polymer multilayer films by electrostatic self-assembly and layer-by-layer post azo functionalization," Macromolecules **33**, 6534–6540 (2000).
[21]A. Garg, R. M. Davis, C. Durak, J. R. Heflin, and H. W. Gibson, "Polar orientation of a pendant anionic chromophore in thick layer-by-layer self-assembled polymeric films," J. Appl. Phys. **104**, 053116 (2008).
[22]J. L. Casson, D. W. McBranch, J. M. Robinson, H. L. Wang, J. B. Roberts, P. A. Chiarelli, and M. S. Johal, "Reversal of interfacial dipole orientation in polyelectrolyte superlattices due to polycationic layers," J. Phys. Chem. B **104**, 11996–12001 (2000).
[23]J. L. Casson, H. L. Wang, J. B. Roberts, A. N. Parikh, J. M. Robinson, and M. S. Johal, "Kinetics and interpenetration of ionically self-assembled dendrimer and PAZO multilayers," J. Phys. Chem. B **106**, 1697–1702 (2002).
[24]G. Aldea-Nunzi, S. W. Chan, K. Y. K. Man, and J. M. Nunzi, "All-optical poling and second harmonic generation diagnostic of layer-by-layer assembled photoactive polyelectrolytes," Chem. Phys. **420**, 7–14 (2013).
[25]G. Aldea, H. Gutiérrez, J.-M. Nunzi, G. C. Chitanu, M. Sylla, and B. C. Simionescu, "Second harmonic generation diagnostic of layer-by-layer deposition from Disperse red 1—Functionalized maleic anhydride copolymer," Opt. Mater. **29**, 1640–1646 (2007).
[26]C. Anceau, S. Brasselet, and J. Zyss, "Local orientational distribution of molecular monolayers probed by nonlinear microscopy," Chem. Phys. Lett. **411**, 98–102 (2005).
[27]B. Park, Y. Kinoshita, T. Sakai, J.-G. Yoo, H. Hoshi, K. Ishikawa, and H. Takezoe, "Determination of orientational distribution function of organic molecular surfaces using the modified maximum-entropy method," Phys. Rev. E **57**, 6717–6724 (1998).
[28]B. Park, H. S. Kim, J. Y. Bae, J. G. Lee, H. S. Woo, S. H. Han, J. W. Wu, M. Kakimoto, and H. Takezoe, "Orientation of a photo-sensitive polymeric monolayer studied by second-harmonic generation," Appl. Phys. B **66**, 445–451 (1998).
[29]S. Schrader, V. Zauls, B. Dietzel, C. Flueraru, D. Prescher, J. Reiche, H. Motschmann, and L. Brehmer, "Linear and nonlinear optical properties of Langmuir–Blodgett multilayers from chromophore-containing maleic acid anhydride polymers," Mater. Sci. Eng. C **8-9**, 527–537 (1999).
[30]Y. W. Yi, T. E. Furtak, M. J. Farrow, and D. M. Walba, "Photoinduced anisotropy of second-harmonic generation from azobenzene-modified alkylsiloxane monolayers," J. Vac. Sci. Technol., A **21**, 1770–1775 (2003).
[31]P. Zhu, M. E. Van der Boom, H. Kang, G. Evmenenko, P. Dutta, and T. J. Marks, "Realization of expeditious layer-by-layer siloxane-based self-assembly as an efficient route to structurally regular acentric superlattices with large electro-optic responses," Chem. Mater. **14**, 4982–4989 (2002).
[32]W. Lin, W. Lin, G. K. Wong, and T. J. Marks, "Supramolecular approaches to second-order nonlinear optical materials. Self-assembly and microstructural characterization of intrinsically acentric [(aminophenyl)azo]pyridinium superlattices," J. Am. Chem. Soc. **118**, 8034–8042 (1996).
[33]H. E. Katz, W. L. Wilson, and G. Scheller, "Chromophore structure, second harmonic generation, and orientational order in zirconium phosphonate/phosphate self-assembled multilayers," J. Am. Chem. Soc. **116**, 6636–6640 (1994).
[34]K. Sahu, K. B. Eisenthal, and F. Mcneil, "Competitive adsorption at the air-water interface: A second harmonic generation study," J. Phys. Chem. C **115**, 9701–9705 (2011).
[35]Y. Niidome, S. Tagawa, and S. Yamada, "Adsorption behaviors of methyl orange to alternate polyion films as studied by *in-situ* absorption and second harmonic generation measurements," Colloids Surf., A **198-200**, 467–472 (2002).
[36]S. A. Mitchell, "Indole adsorption to a lipid monolayer studied by optical second harmonic generation," J. Phys. Chem. B **113**, 10693–10707 (2009).
[37]G. J. Ashwell, T. W. Walker, and P. Leeson, "Improved second-harmonic generation from langmuir-blodgett films," Langmuir **14**, 1525–1527 (1998).
[38]P. Hedge, Z. Ali-Adib, D. West, and T. King, "Efficient second-harmonic generation from thick all-polymeric langmuir-blodgett films," Macromolecules **26**, 1789–1792 (1993).
[39]J. R. Heflin, C. Figura, D. Marciu, Y. Liu, and R. O. Claus, "Thickness dependence of second-harmonic generation in thin films fabricated from ionically self-assembled monolayers," Appl. Phys. Lett. **74**, 495–497 (1999).
[40]Y. R. Shen, "Surfaces probed by nonlinear optics," Surf. Sci. **299/300**, 551–562 (1994).
[41]R. W. Boyd, *Nonlinear Optics*, 2nd ed. (Academic Press, New York, 2004).
[42]Y. R. Shen, in *The Principles of Nonlinear Optics*, 1st ed. (Academic Press, San Diego, CA, 1988), Chap. 25.
[43]A. G. Lambert, P. B. Davis, and D. J. Neivandt, "Implementing the theory of sum frequency generation vibrational spectroscopy: A tutorial review," Appl. Spectrosc. Rev. **40**, 103–145 (2005).
[44]M. B. Feller, W. Chen, and Y. R. Shen, "Investigation of surface-induced alignment of liquid-crystal molecules by optical second-harmonic generation," Phys. Rev. A **43**, 6778–6792 (1992).
[45]F. J. S. Lopes, "Estudo da orientação molecular em filmes automontados de azopolímeros por meio da técnica de geração de segundo harmônico (SHG)," M.S. dissertation, University of São Paulo, São Carlos, Brazil, 2006 http://www.teses.usp.br/teses/disponiveis/88/88131/tde-18122006-161256/pt-br.php.
[46]B. Jérôme and Y. R. Shen, "Anchoring of nematic liquid crystals on mica in the presence of volatile molecules," Phys. Rev. E **48**, 4556–4574 (1993).
[47]X. Zhuang, "Nonlinear optical studies of liquid crystals and polymers," Ph.D. thesis, University of California, Berkeley, 1996.
[48]W. Chen, "Linear and nonlinear optical studies of liquid crystals interfaces," Ph.D. thesis, University of California, Berkeley, 1996.
[49]N. C. De Sousa, V. Zucolotto, J. R. Silva, D. S. Santos, Jr., O. N. Oliveira, Jr., and J. A. Giacometti, "Morphology characterization of layer-by-layer films from PAH/MA-co-DR13: The role of film thickness," J. Colloid Interface Sci. **285**, 544–550 (2005).
[50]H. S. Silva, T. M. Uehara, K. Bergamaski, and P. B. Miranda, "Molecular ordering in layer-by-layer polyelectrolyte films studied by sum-frequency vibrational spectroscopy: The effects of drying procedures," J. Nanosci. Nanotechnol. **8**, 3399–3405 (2008).
[51]X. Zhuang, P. B. Miranda, D. Kim, and Y. R. Shen, "Mapping molecular orientation and conformation at interfaces by surface nonlinear optics," Phys. Rev. B **59**(19), 12632–12640 (1999).
[52]S. Cattaneo, K. Miettinen, E. Vuorimaa, H. Lemmetyinen, and M. Kauranen, "Linear optics in the second-order characterization of thin films," Chem. Phys. Lett. **419**, 492–495 (2006).
[53]R. Superfine, J. Y. Huang, and Y. R. Shen, "Phase measurement for surface infrared–visible sum-frequency generation," Opt. Lett. **15**, 1276–1278 (1990).
[54]H. S. Silva and P. B. Miranda, "Molecular ordering of layer-by-layer polyelectrolyte films studied by sum-frequency vibrational spectroscopy," J. Phys. Chem. B **113**, 10068–10071 (2009).